Molecular modeling and simulation of polyamide membrane for forward osmosis process

Jester N. Itliong[1]*, Joaquin Lorenzo V. Moreno[1,2], Al Rey C. Villagracia[1,2], Melanie Y. David[1,2], and Nelson B. Arboleda, Jr.[1,2,3]

[1] Physics Department, College of Science, De La Salle University, 2401 Taft Ave., Malate, 1004 Manila
[2] ANIMoS Research Unit, CENSER, De La Salle University, 2401 Taft Ave., Malate, 1004 Manila
[3] De La Salle University - Science and Technology Complex, Biñan, Laguna
*Corresponding Author: jester_itliong@dlsu.edu.ph

Abstract: As a first step in studying the molecular-level water transport and reverse solute diffusion mechanisms in forward osmosis (FO) process, this paper presents the molecular modeling and simulation of a polyamide (PA) membrane used in FO. In this study, a repeat unit of the starting monomers (*m*-phenylenediamine (MPD) and trimesoyl chloride (TMC)) was first modeled and then packed into chain, forming a linear PA chain. Geometry optimization and partial charge calculations of the linear PA chain were undergone using Density Functional Theory (DFT) calculations. A fully atomistic molecular dynamics (MD) simulation of the PA chains was performed to create a final representative model of PA membrane. The generated dehydrated and linear (un-crosslinked) PA membrane structure obtained a density value which is in close agreement with recent experimental and other simulation results. In addition, the calculated small-angle x-ray scattering intensities show that the obtained PA membrane structure is indeed amorphous. The amorphous structure of the membrane is believed to be due to the annealing scheme in the simulation which removed the lattice periodicity from the initial structure of the membrane.

Key Words: polyamide; molecular dynamics; forward osmosis

1. INTRODUCTION

Pressure driven membrane processes such as that of reverse osmosis (RO) are commercially used today for water treatment, desalination, and water purification. The process relies on the application of high pressures to drive seawater (or wastewater) through a selectively permeable membrane, therefore rejecting salt ions and other particles while allowing water to pass through (Dupont et al., 1982). An example of a membrane that has been widely accepted and utilized in RO is a thin-film composite

(TFC) membrane made of a thin aromatic polyamide (PA) active layer and a much thicker polysulfone (PSf) support layer. PA is formed via interfacial polymerization (IP) of *m*-phenylene diamine (MPD) and trimesoyl chloride (TMC; 1,3,5-tricarboxylic acid chloride) in aqueous phase and organic phase, respectively, at the surface of microporous PSf (Kwak and Ihm, 1999). The dense and complex structure of the PA layer is responsible for salt rejection while PSf provides mechanical strength to the membrane.

The PA membrane under RO conditions provides reliable performance in terms of selectivity and water permeability (Eriksson, 1988). However, the process itself is relatively energy intensive since it requires high pressure to operate (Dashtpour and Al-Zubaidy, 2012). Forward osmosis (FO), an emerging and promising alternative to RO, is gaining attention for its potential to overcome the drawbacks in RO. Unlike RO and other pressure driven membrane processes, FO uses the natural osmotic pressure generated by the draw solutions (e.g. NaCl) as a driving force for water to transport through the membrane (Cath et al., 2006). Initial studies on FO processes were started by testing RO membranes under FO operating conditions and recently, attempts to develop new appropriate membranes have been worked out (Cath et al., 2006; Zhao et al., 2012). Furthermore, owing to the low or no hydraulic pressures requirement, FO exhibits potential advantages in terms of energy and separation efficiency as compared to RO (Zhao et al., 2012). With this, FO has been applied in many applications such as in landfill leachate dewatering, of industrial wastewater (Zhang et al., 2014), sludge dewatering (Eusebio et al., 2008), and microalgae dewatering (Larronde-Larretche and Jin, 2016).

In spite of the promise, FO technology is still in its early stage of development and some important mechanisms are largely unknown (Cath et al., 2006). For example, the mechanisms of water and salt transport through PA membrane in RO process were studied experimentally (Roh et al., 2006) and details on the molecular mechanisms were understood through modeling and simulations (Kotelyanskii et al., 1999; Harder et al., 2009), yet these are not currently studied in FO process. Essentially, the occurence of reverse solute diffusion (i.e. back diffusion of salts from the draw solution to the surface and inside of the membrane during FO) and its relationship to water permeability are of particular interests to investigate. Inspired by the success of the previous simulation works that advanced the understanding of PA membranes and RO process, the authors of this paper proposed to study the molecular level water transport and reverse solute diffusion mechanisms across a PA membrane during FO using Molecular Dynamics (MD) simulations.

As an initial undertaking, this paper presents the molecular modeling and simulation of a PA membrane used in FO. In this study, a DFT- and MD-based method for producing a molecular model of PA membrane is demonstrated. From the simulations, structural properties such as density and amorphicity were derived, which are found to be in fair agreement with experimental values. The obtained model will be used in studying the fundamental mechanisms in FO and it is hoped that this work will contribute to the development of FO membranes and the FO technology as well.

2. THEORY: Molecular Dynamics

MD is a computational method that employs Newton's equations of motion to simulate the time evolution of a system of particles such as their positions, velocities, forces, and trajectories. It offers a physical basis in understanding the structure, function, dynamics, interactions, and mechanisms of biomolecules and some materials (Karplus and McCammon, 2002). MD depends on the knowledge of the approximate empirical interaction potential for the particles (the force field). A force field is a functional expression that consists of intramolecular (bond stretching, angle bending, dihedral, and improper torsions) and intermolecular (Van der Waals and Coulombic interactions) contributions to the total potential energy U ($\mathbf{r}_1$, $\mathbf{r}_2$, . . . ,$\mathbf{r}_N$), of the system of particles under study. It must also contain a set of parameters or constants that are usually obtained either from experiments or *ab initio* quantum mechanical calculations or from a combination of both.

Expressions for force fields may vary depending on the degree of complexity and the type of system one wishes to study, but a typical expression for a force field (or the force field used by the software employed in this study) is given by (Gonzalez, 2011):

$$U = \sum_{bonds} \frac{1}{2} k_b (r - r_0)^2 + \sum_{angles} \frac{1}{2} k_a (\theta - \theta_0)^2 + \sum_{torsions} \frac{V_n}{2} [1 + \cos(n\phi - \delta)]$$

$$+ \sum_{improper} V_{imp} + \sum_{LJ} 4\epsilon_{ij} \left[\left(\frac{\sigma_{ij}}{r_{ij}}\right)^{12} - \left(\frac{\sigma_{ij}}{r_{ij}}\right)^6 \right] + \sum_{Coulomb} f \frac{q_i q_j}{\epsilon_r r_{ij}} \quad \text{(Eq.1)}$$

Bond stretching — Angle bending — Dihedral torsion — Improper torsion — LJ potential (Van der Waals) — Coulomb (Electrostatics)

where:

U	=	potential energy
k_b	=	harmonic bond force constant
r	=	actual bond stretch
r_o	=	equilibrium bond length
k_a	=	harmonic angle bending constant
θ	=	actual bond angle
θ_o	=	reference bond angle
V_n	=	torsional rotation force constant
Φ	=	current torsional angle
δ	=	phase angle
V_{imp}	=	improper torsion force constant
ϵ_{ij}	=	strength of interaction
σ_{ij}	=	closest distance approach
r_{ij}	=	distance between atoms i and j
f	=	permittivity of free space
$q_i q_j$	=	charged particles
ϵ_r	=	relative dielectric constant

By solving for the negative gradient of the potential energy given above, the forces acting on the particles can be obtained, and thus the equations of motion of the particles (Karplus and Petsko, 1990). Using MD, the system under observation can be probed more easily than in experiments, and therefore provides answer to specific questions about the mechanisms and properties of a system (Karplus and Petsko, 1990; Karplus and McCammon, 2002).

3. METHODS

The polymerization process of MPD and TMC monomers can produce polymer chains that are either cross-linked or linear. Cross-linked chains are formed when one polymer chain covalently bond to another polymer chain (IUPAC, 1996) while linear

chains (also called polymer melt) are chains that are overlapping but not cross-linked. Fig. 1 shows the chemical structures of the starting MPD and TMC monomers considered in this study and the resulting PA chains when they undergo polymerization.

Given that there is insufficient accurate information about the complex chemical and network structure of PA membrane (since only density and morphology were successfully characterized by experiments), it is quite challenging to create a model that will exactly represent it. On the time scale of MD simulations, the polymerization process that produces a fully cross-linked PA membrane is prohibitively slow (Harder et al., 2009). In addition, standard membrane-modeling strategy has yet to be established. Thus to reduce computational cost, while not sacrificing the quality of results to be obtained, this study adopted the method used by Xiang et al., 2013 and Gao et al., 2015, where linear PA membrane is built and cross-linking is not considered. Also, this work excludes the PSf support layer in the system and only focuses on PA active layer since it is the one responsible for salt rejection and water permeability.
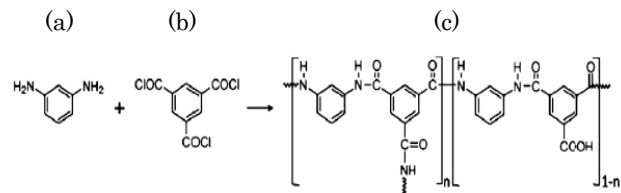

(a)　　(b)　　(c)

Fig. 1. Representative chemical structures of (a) MPD, (b) TMC, and (c) PA chain (cross-linked and linear chains can be determined on the degree of cross-linking n, which can take values between 0 and 1, with $n = 0$ for linear chains only and $n = 1$ for a fully cross-linked polymer chain (Ding et al., 2014))

3.1 Linear PA chain model

Given the reference structure in Fig. 1(c), where $n = 0$, a linear PA chain consisting of three repeated PA units (Fig. 2) was modeled using the Materials Studio software (BIOVIA). The atomic arrangement in the repeat unit shows that two carboxylate groups of TMC monomers were covalently bonded to the amino group of MPD monomers, therefore obtaining amide bonds. The generated single linear PA chain is thus composed of

6 MPD and 6 TMC monomers with a corresponding chemical formula $C_{90}H_{54}N_{12}O_{25}$.

To guarantee the structural stability of the PA chain, geometry optimization was performed by Density Functional Theory (DFT) calculation at PBE level with *dnd* basis set under the Dmol3 package in Materials Studio software. Calculations of the chain's partial atomic charges were also carried out by means of Mulliken charge analysis.

The topological information (i.e. a file containing the complete description of interactions in the system such as the force field parameters and constants) of the successfully optimized linear PA chain model was generated using PRODRG (Schuttelkopf and van Aalten, 2004) for use in MD simulations. However, the parameters for partial atomic charges produced by PRODRG were replaced by the charges obtained from Mulliken analysis. This is due to the incompatibility of the PRODRG-obtained charges with the GROMOS force field (Lemkul et al., 2010) used in this study.
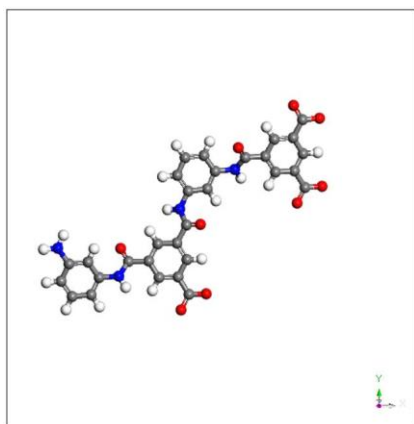

Fig. 2. The repeat unit in linear PA chain molecule. Carbon (dark grey), Hydrogen (white), Nitrogen (blue), Oxygen (red).

3.2 PA membrane construction

To finally build the PA membrane, MD simulations were performed using the software GROMACS (GROningen Machine for Chemical Simulations; Bekker et al., 1993) with GROMOS53a6 (Oostenbrink et al., 2004) as the force field. The interaction potentials in this force field were generally described in the Theory section. Prior to actual MD simulations, energy minimization (EM)

and equilibration (constant NVT: number of atoms, volume, and temperature; and constant NPT: number of atoms, pressure, and temperature) were undergone to the system. The steepest descent algorithm was utilized for EM which ensured that the system is close to equilibrium. The V-rescale thermostat (Bussi et al., 2007) was used in NVT for control of the temperature and Berendsen barostat (Berendsen et al., 1984) was used in NPT for pressure control. Moreover, LINCS (Hess et al., 1997) was used as an algorithm for holonomic bond contraints and long-range electrostatic interactions were manipulated by PME (Essmann et al., 1995).

At the start of the simulations, a controlled random insertion of linear PA chains into a simulation box was implemented through the *gmx insert-molecules* command in GROMACS. The controlled insertion takes place by initially putting small number of chains in the box (5 chains) and performing EM at 50 ps and equilibration at 1000 ps to the system. Equilibration maintained the temperature to 300 K and the pressure to 1 bar. The simulation box (xyz vectors) of the equilibrated system is then increased and additional PA chains are inserted. Another round of EM and equilibration were undergone in this new conformation of PA chains. This process continued until the energy of the system is no longer possible to be minimized. Due to this, a total of 128 linear PA chains were successfully inserted, energy minimized, and equilibrated. This strategy allowed careful control of the density of the system to reach a target dehydrated PA membrane density value of 1.06 g/cm^3 (Mi et al., 2007). The method also warranted that no steric clashes and unwanted large forces will be present in the system.

The actual MD simulation was done by annealing the equilibrated conformation of PA chains. This is made possible by means of *simulated annealing* option in GROMACS where annealing is performed by dynamically (but not instantaneously) changing the reference temperature of the system at a specified simulation time. The simulated annealing scheme used in obtaining the final PA membrane model consists of heating the system up to 600 K at the start of the simulation, and linearly cooling it down to 300 K at 4000 ps where it remains constant until the end of simulation (at 5000 ps). After 5000 ps MD simulation, a representative linear and dehydrated PA membrane model (Fig. 3) was generated inside a box with the final dimensions of 6.4 nm × 6.4 nm × 8.0 nm.
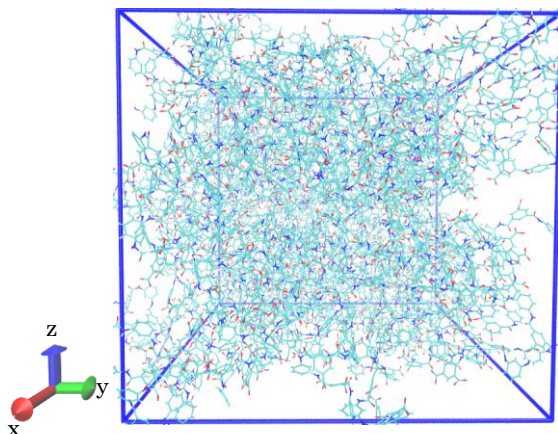
Fig. 3. A snapshot (in perspective view) of the fully linear and dehydrated PA membrane after the MD simulation (annealing scheme). Carbon (cyan), Hydrogen (white), Nitrogen (blue), Oxygen (red).

Fig. 4. Density profile of the fully linear and dehydrated PA membrane.

4. RESULTS AND DISCUSSION

The resulting final conformation of the PA membrane allows important properties to be calculated, analysed, and compared. Fig. 4 shows the calculated partial density profile of the PA membrane across the z-axis of the simulation box. The graph shows that starting from 2 nm up to 6 nm, the density remains close between 1000 and 1100 kg/m^3. The average system density was found to be 1085.04 kg/m^3 (or 1.085 g/cm^3), near the experimental value of 1.06 g/cm^3 for dehydrated PA membrane and in fair agreement with previous simulation works (Gao et al., 2015; Xiang et al., 2013) on fully linear PA membrane.

Furthermore, to provide some insights on the behaviour of the system during the annealing scheme, the system's temperature and density as a function of simulation time were calculated and are shown in Fig. 5. As seen in Fig. 5(a), the system is heated starting at 600 K and the temperature linearly drops to 300 K at 4000 ps which remain constant until the simulation is over. Consequently, Fig. 5(b) indicates the increasing amount of the average system density as the simulation runs. It can then be noted that the density started to become stable at 4000 ps.

By extracting both the temperature and density information as shown in Fig. 5 and plotting them into a graph (Fig. 6) we can see clearly the
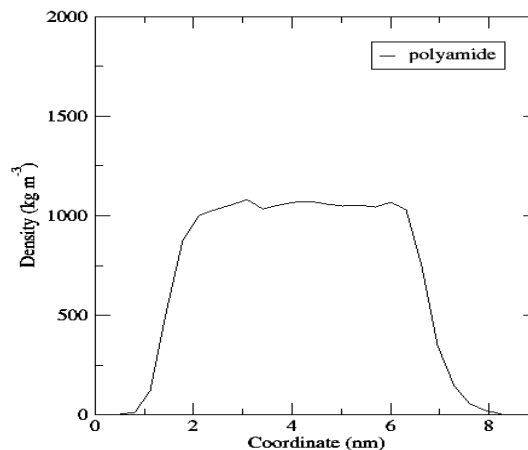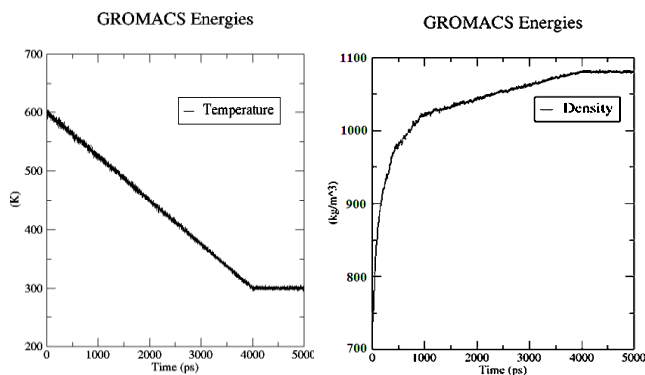

Fig. 5. (a) System temperature and (b) average density during the annealing scheme.
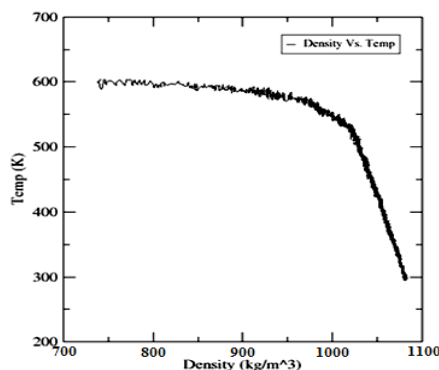
Fig. 6. The effect of temperature to the density of the system.

relationship between the two and we can further explain how the system reached its final density. Fig. 6 shows the inverse proportionality of density to temperature. It implies that as the temperature of the system decreases, the density increases. By theory it is known that the temperature has a direct relationship with the kinetic energy of the system and therefore to the velocity of the particles in the system. Thus a decreasing temperature corresponds to a decreasing velocity which then results to minimize movements of the particles. This minimized movements of the particles as well as the simultaneous compression of volume in the system draw the particles (or the PA chains) closer together leading to an increase in the PA membrane density.

Lastly, the calculated small-angle x-ray scattering intensities (Fig. 7) shows that the obtained linear PA membrane structure is indeed amorphous. Higher scattering (peak) is observed between 0 to 5 nm^{-1} regions, which is the same result obtained by a previous experimental work (Silva et al., 2015). The amorphous structure is also agreeable with the simulation work by Kotelyanskii et al., 1998. The amorphous structure of the membrane is believed to be due to the annealing scheme in the simulation which removed the lattice periodicity from the initial structure of the membrane.
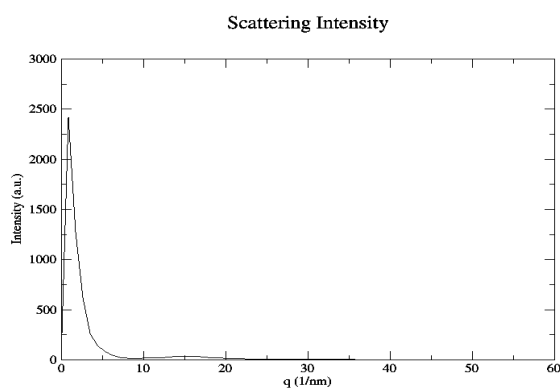

Fig. 7. Calculated small-angle x-ray scattering intensity of the PA membrane.

5. CONCLUSIONS

Molecular model of a fully linear and dehydrated PA active layer membrane had been created with density and structure that closely resemble that of experimental and other simulation values. The results are mainly attributable to the annealing scheme in the simulation which allowed the PA membrane to be denser than its previous equilibrated conformation. The simulation also reconfigured the position and orientation of the PA chains resulting to an amorphous cell of PA membrane.

The consistency of the results also guaranteed the validity of the force field and the parameters used (specifically that of DFT-calculated partial atomic charges). The careful yet effective strategy of inserting PA chains inside the simulation box was found to be helpful in maintaining the stability of the system. It has also paved a way for controlling the density of the system to obtain a target final density value.

Calculations of other properties such as the pore size distribution inside the membrane and density-mapping would provide better quantitative and qualitative understanding on the structure of the membrane. These are currently reserved for future works or may also be studied by other researchers. The obtained model will then be used in the simulations of FO process where the mechanisms of water transport and reverse solute diffusion across the PA membrane will be investigated. It is hoped that this study will contribute to the existing knowledge and development of FO membranes and the FO technology as well.

6. ACKNOWLEDGMENTS

7. REFERENCES

Bekker, H., Berendsen, H. J. C., Dijkstra, E. J., Achterop, S., van Drunen, R., van der Spoel, D., Sijbers, A., Keegstra, H., Reitsma, B., & Renardus, M. K. R. (1993) Gromacs: A parallel computer for molecular dynamics simulations. Physics Computing, 92.

Berendsen, H. J. C., Postma, J. P. M., van Gunsteren, W. F., DiNola, A., & Haak, J. R. (1984). Molecular dynamics with coupling to an external bath. The Journal of Chemical Physics, 81, 3684.

Bussi, G., Donadio, D., & Parrinello, M. (2007). Canonical sampling through velocity rescaling. The Journal of Chemical Physics 126 (1), 014101-1–014101-7.

Cath, T. Y., Childress, A. E., & Elimelech, M. (2006). Forward osmosis: principles, applications, and recent developments. Journal of Membrane Science, 281, 70–87.

Dashtpour, R. & Al-Zubaidy, S. N. (2012). Energy Efficient Reverse Osmosis Desalination Process. International Journal of Environmental Science and Development, 3, No. 4.

Ding, M., Ghoufi, A., & Szymczyk, A. (2014). Molecular simulations of polyamide reverse osmosis membranes. Desalination, 343, 48–53.

Dupont, R. R., Eisenberg, T. N., & Middlebrooks, E. J. (1982). Reverse Osmosis in the Treatment of Drinking Water. Reports, 505.

Eriksson, P. (1988). Water and salt transport through two types of polyamide composite membranes. Journal of Membrane Science, 36, 297–313.

Essmann, U., Perera, L., & Berkowitz, M. L. (1995). A smooth particle mesh Ewald method. The Journal of Chemical Physics, 103, 8577.

Eusebio, R. C., Kim, H. G., & Kim, H. S. (2008). Application of MF Membrane in Sludge Reduction System. Korean Society of Water and Environment, Joint Autumn Conference, 63-64.

Gao, W., She, F., Zhang, J., Dumée, L. F., He, L., Hodgson, P. D., & Kong, L. (2015). Understanding water and ion transport behavior and permeability through poly(amide) thin film composite membrane. Journal of Membrane Science, 487, 32–39.

Gonzalez, M. A. (2011). Force fields and molecular dynamics simulations. Collection SFN, 12, 169–200.

Harder, E., Eric Walters, D., Yaroslav, D., Bodnar, R., Faibish, S., & Roux, B. (2009). Molecular Dynamics Study of a Polymeric Reverse Osmosis Membrane. Journal of Physical Chemistry B, 113, 10177–10182.

Hess, B., Bekker, H., Berendsen H. J. C., & Fraaije, J. G. E. M. (1997). LINCS: a linear constraint solver for molecular simulations. Journal of Computational Chemistry, 18, 1463-1472.

IUPAC (1996). Glossary of basic terms in polymer science. Pure and Applied Chemistry 68 (12), 2287–2311.

Karplus, M., & Petsko G. A. (1990). Molecular dynamics simulations in biology. Nature London, 631-639.

Karplus, M., & McCammon, J. A. (2002). Molecular dynamics simulations of biomolecules. Nature Structural Biology, 9, 646-652.

Kotelyanskii, M. J., Wagner, N. J., & Paulaitis, M. E. (1998). Atomistic simulation of water and salt transport in the reverse osmosis membrane FT-30. Journal of Membrane Science, 139, 1-16.

Kotelyanskii, M. J., Wagner, N. J., & Paulaitis, M. E. (1999). Molecular dynamics simulation study of the mechanisms of water diffusion in a hydrated, amorphous polyamide. Computational and Theoretical Polymer Science, 9, 301–306.

Kwak, S. -Y. & Ihm, D. W. (1999). Use of atomic force microscopy and solid-state NMR spectroscopy to characterize structure-property-performance correlation in high-flux reverse osmosis (RO) membranes. Journal of Membrane Science, 158, 143 – 153.

Larronde-Larretche, M., & Jin, X. (2016). Microalgae (Scenedesmus obliquus) dewatering using forward osmosis membrane: Influence of draw solution chemistry. Algal Research, 15, 1–8.

Lemkul, J. A., Allen, W. J., & Bevan, D. R. (2010). Practical Considerations for Building GROMOS-Compatible Small-Molecule Topologies. J. Chem. Inf. Model, 50 (12), 2221–2235.

Mi, B. X., Cahill, D. G., & Marinas, B. J. (2007) Physico-chemical integrity of nanofiltration/reverse osmosis membranes during characterization by Rutherford backscattering spectrometry. Journal of Membrane Science, 291 (1-2), 77-85.

Oostenbrink, C., Villa, A., Mark, A. E., & Van Gunsteren, W.F. (2004). A biomolecular force field based on the free enthalpy of hydration and solvation: The GROMOS force-field parameter sets 53A5 and 53A6. Journal of Computational Chemistry, 25 (13), 1656–1676.

Roh, I. J., Greenberg, A. R., & Khare, V. P. (2006). Synthesis and characterization of interfacially polymerized polyamide thin films. Desalination, 191, 279–290.

Schuttelkopf, A. W., & van Aalten, D. M. F. (2004). PRODRG: a tool for high-throughput crystallography of protein-ligand complexes. Acta Crystallography D, 60, 1355-1363.

Silva, R. C., Ortiz-Medina, J., Morelos-Gomez, A., Inukai, S., Takeuchi, K., Kawaguchi, T., Hayashi, T., & Endo, M. (2015). Carbon

nanotube/polyamide membranes: a SAXS study. Experiments, 201501014.

Xiang, Y., Liu, Y., Mi, B., & Leng Y. (2013). Hydrated Polyamide Membrane and Its Interaction with Alginate: A Molecular Dynamics Study. Langmuir, 29 (37), 11600–11608.

Zhang, X., Ning, Z., Wang, D.K., & Diniz da Costa, J.C. (2014). Processing municipal wastewaters by forward osmosis using CTA membrane. Journal of Membrane Science, 468, 269–275.

Zhao, S., Zou, L., Tang, C. Y., & Mulcahy, D. (2012). Recent developments in forward osmosis: Opportunities and challenges. Journal of Membrane Science, 396, 1– 21.